OPEN

Molecular Psychiatry (2016) 21, 1561–1572

www.nature.com/mp

ORIGINAL ARTICLE

Misassembly of full-length Disrupted-in-Schizophrenia 1 protein is linked to altered dopamine homeostasis and behavioral deficits

SV Trossbach[1,13], V Bader[1,13], L Hecher[1], ME Pum[2], ST Masoud[3], I Prikulis[1], S Schäble[2,14], MA de Souza Silva[2], P Su[4], B Boulat[5], C Chwiesko[5], G Poschmann[6], K Stühler[6], KM Lohr[7], KA Stout[7], A Oskamp[8], SF Godsave[9], A Müller-Schiffmann[1], T Bilzer[1], H Steiner[10], PJ Peters[9,15], A Bauer[8], M Sauvage[5], AJ Ramsey[3], GW Miller[7], F Liu[4], P Seeman[11], NJ Brandon[12], JP Huston[2] and C Korth[1]

Disrupted-in-schizophrenia 1 (*DISC1*) is a mental illness gene first identified in a Scottish pedigree. So far, DISC1-dependent phenotypes in animal models have been confined to expressing mutant DISC1. Here we investigated how pathology of full-length DISC1 protein could be a major mechanism in sporadic mental illness. We demonstrate that a novel transgenic rat model, modestly overexpressing the full-length *DISC1* transgene, showed phenotypes consistent with a significant role of DISC1 misassembly in mental illness. The tgDISC1 rat displayed mainly perinuclear DISC1 aggregates in neurons. Furthermore, the tgDISC1 rat showed a robust signature of behavioral phenotypes that includes amphetamine supersensitivity, hyperexploratory behavior and rotarod deficits, all pointing to changes in dopamine (DA) neurotransmission. To understand the etiology of the behavioral deficits, we undertook a series of molecular studies in the dorsal striatum of tgDISC1 rats. We observed an 80% increase in high-affinity DA D2 receptors, an increased translocation of the dopamine transporter to the plasma membrane and a corresponding increase in DA inflow as observed by cyclic voltammetry. A reciprocal relationship between DISC1 protein assembly and DA homeostasis was corroborated by *in vitro* studies. Elevated cytosolic dopamine caused an increase in DISC1 multimerization, insolubility and complexing with the dopamine transporter, suggesting a physiological mechanism linking DISC1 assembly and dopamine homeostasis. DISC1 protein pathology and its interaction with dopamine homeostasis is a novel cellular mechanism that is relevant for behavioral control and may have a role in mental illness.

Molecular Psychiatry (2016) **21,** 1561–1572; doi:10.1038/mp.2015.194; published online 12 January 2016

INTRODUCTION

Disrupted-in-schizophrenia 1 (*DISC1*) is a gene involved in vulnerability to behavioral disorders. It was discovered in a large Scottish pedigree with a chromosomal translocation leading to a 3′ truncation of the *DISC1* gene and, putatively, a C-terminal truncation of the resulting protein.[1] In this family, the translocation is associated with several major clinical diagnoses such as schizophrenia, recurrent major depression and bipolar disorder.[1–3] Subsequent genetic association studies in multiple populations of different ethnicities support the involvement of DISC1 in mental illnesses (reviewed in refs. 4,5). For example, the coding polymorphisms S704C (rs821616) and L607F (rs6675281) in *DISC1* were associated with mental illness and also showed increased DISC1 protein aggregation *in vitro*.[6,7] In parallel, various transgenic or genetically altered mouse models have been developed, either targeting the mouse *Disc1* locus or introducing mutant human DISC1 variants. Missense mutations,[8] deletion variants[9,10] or partial knockout of the endogenous mouse *Disc1* locus[11] were generated. In addition, the dominant-negative truncated form of human DISC1, which is thought to correspond to the truncated *DISC1* gene in the Scottish family, was also induced[12] or constitutively[13] expressed in mouse models. Together these studies have provided evidence of DISC1 being involved in neurodevelopment and behavioral control.[14]

Thus far, DISC1 mouse models have been used to investigate the role of genetically altered or silenced DISC1 in behavioral control rather than the full-length form present in all sporadic cases of chronic mental illness that may, at least in part, underlie the etiology of the disorder.

[1]Department Neuropathology, Medical Faculty, Heinrich Heine University Düsseldorf, Düsseldorf, Germany; [2]Center for Behavioral Neuroscience, Heinrich Heine University Düsseldorf, Düsseldorf, Germany; [3]Department of Pharmacology and Toxicology, University of Toronto, Toronto, Ontario, Canada; [4]Campbell Family Mental Health Research Institute, Centre for Addiction and Mental Health, Toronto, Ontario, Canada; [5]Functional Architecture of Memory Unit, Mercator Research Group, Faculty of Medicine, Ruhr University Bochum, Bochum, Germany; [6]Molecular Proteomics Laboratory, BMFZ, Heinrich Heine University Düsseldorf, Düsseldorf, Germany; [7]Department of Environmental Health, Rollins School of Public Health, Emory University, Atlanta, GA, USA; [8]Institute of Neuroscience and Medicine, INM-2, Forschungszentrum Jülich, Jülich, Germany; [9]The Netherlands Cancer Institute, Amsterdam, The Netherlands; [10]Department of Cellular and Molecular Pharmacology, The Chicago Medical School, Rosalind Franklin University of Medicine and Science, North Chicago, IL, USA; [11]Departments of Pharmacology and Psychiatry, University of Toronto, Toronto, Ontario, Canada and [12]AstraZeneca Neuroscience iMED, Cambridge, MA, USA. Correspondence: Professor C Korth, Neurodegeneration Unit, Department Neuropathology, University of Düsseldorf Medical School, Moorenstrasse 5, 40225 Düsseldorf, Germany.
E-mail: ckorth@hhu.de
[13]These authors contributed equally to this work.
[14]Current address: Comparative Psychology, Heinrich Heine University Düsseldorf, Germany.
[15]Current address: The Maastricht Multimodal Molecular Imaging Institute, Maastricht University, Maastricht, The Netherlands.
Received 14 November 2014; revised 16 October 2015; accepted 22 October 2015; published online 12 January 2016

The fact that *DISC1* has not yet been identified among the major GWAS hits has raised controversies[15,16] even though it merely indicates that *DISC1* is not targeted by common risk variants. It has been pointed out that the study of rare gene variants may provide valuable insights into disease mechanism. One such example is Alzheimer's disease (AD) where common mutations in the major disease genes *APP* and the presenilins also do not appear in GWAS screens[17] even though APP processing is a critical step in AD pathogenesis.

Genetic association, however, is only one way to address the connection between a disease and its biological cause. Investigations of the protein itself can also validate its role in non-familial forms of a brain disease. For example, protein pathology is a major biological cause for most chronic brain diseases such as AD, frontotemporal dementias or Parkinson's disease in which a dysfunctional proteostatic system leads to the accumulation of disease-specific protein aggregates.[18] Remarkably, in these diseases the same proteins accumulate in sporadic forms as well as familial genetic forms where these proteins are mutated.[18] Furthermore, accumulation of proteins is a controlled process in the cell that is even used to generate functional aggregates in physiological circuitry.[19]

In this study, we asked whether non-mutant, full-length DISC1 could have a role in sporadic chronic mental illness including schizophrenia and recurrent affective disorders. Specifically, we investigated whether protein pathology or misassembly of DISC1 could have a role in causing mental illness. Our initial investigations using biochemical techniques identified insoluble DISC1 in a subset of mental illness patients,[20] leading to both gain and loss of function interactions.[20,21]

Although both cellular and animal studies linked DISC1 to various neurotransmitter systems,[22] including the dopaminergic system,[23–28] the actual role of DISC1 in altering dopamine signaling was not elucidated to molecular detail. Of note, in the rodent and human brains, formation of a functional complex between DISC1 and postsynaptic dopamine 2 receptors (D2R) has been demonstrated.[29]

Here to mimic DISC1 protein misassembly, non-mutant full-length human DISC1 was modestly overexpressed as a transgene in Sprague Dawley rats (tgDISC1 rats). Extensive neurochemical, biochemical and behavioral analyses demonstrate a signature of behavioral phenotypes including amphetamine supersensitivity, hyperexploratory behavior and rotarod deficits. These phenotypes are attributable to: (1) a switch of low affinity to high affinity dopamine D2 receptors and (2) increased clearance of extracellular dopamine due to translocation of the dopamine transporter (DAT) in the dorsal striatum (dStr) of tgDISC1 rats. A reciprocal relationship between DISC1 aggregation and dopamine homeostasis suggests that DISC1 may act as a sensor of cytosolic oxidative stress. Regulation of DISC1 assembly through environmental insults may therefore impact dopamine homeostasis.

MATERIALS AND METHODS

Generation of the DISC1 transgenic rat

Transgenic Sprague Dawley rats were generated by injecting the linearized fragment of the CosSHa.tet vector[30] containing the full-length, non-mutant human DISC1 as transgene with the polymorphisms F607 and C704 into pronuclei of Sprague Dawley rats (contracted to the IBZ University of Heidelberg, Germany). Integration of the transgene in the genome of the resulting litters was confirmed in independent founder animals by PCR and Southern blotting of genomic DNA extracted from tail biopsies. Subsequent breeding with wild type Sprague Dawley rats excluded transgenic founders that did not carry the transgene in their germline. By quantitative RT-PCR of genomic DNA and western blotting of brain homogenate the transgene load as well as expression level was compared between the four resulting stable founder lines.

Transgene detection by PCR and qPCR

Genomic DNA was prepared by digesting tail biopsies in 100 mM Tris pH 8, 5 mM EDTA, 0.2% SDS, 200 mM NaCl and 100 μg ml^{-1} Proteinase K, precipitation with isopropanol and solubilization in pure water.

PCR for the detection of the transgene was performed on the genomic DNA by utilizing the HotStarTaq (Qiagen, Hilden, Germany) and primers binding the transgene promoter region: forward 5′-CTGATCTCCAGAAGC CCAAA-3′, reverse 5′-CAGGCCTATTCCTTGACAGC-3′. For the quantitative real-time PCR the same primers for the transgene were used. For normalization primers targeting the genomic sequence of the housekeeping gene rat beta-actin were designed: forward 5′-GCAACGCGCAGCCACTGTCG-3′, reverse 5′-CCACGCTCCACCCCTCTAC-3′. Real-Time PCR was conducted with the StepOnePlus Real-Time PCR System (Applied Biosystems, Carlsbad, CA, USA) and the Platinum SYBR Green qPCR SuperMix-UDG (Invitrogen, Carlsbad, CA, USA). PCR conditions: 10 min at 95 °C, then 40 cycles of 15 s at 95 °C and 60 °C for 1 min. The data were processed with the corresponding StepOne Software v2.3 (Thermo Fisher Scientific, Waltham, MA, USA) and DISC1 expression was normalized to expression level of beta-actin.

Animals and behavioral analyses

All experiments were conducted in conformity with the Animal Protection Law approved by local authorities (LANUV NRW, Recklinghausen, Germany). Male tgDISC1 rats (transgenic rat; TG), negative controls (NC) and Wistar rats were bred in the Animal Facility at the University of Düsseldorf, Germany. NCs were bred from constantly renewed transgene-negative offspring. Male homozygous tgDISC1 rats of founder line 3, but also line 1, non-transgenic littermates and NCs were used for the experiments presented. Experiments were mainly performed in founder line 3, but main results were validated in founder line 1. Rats were housed three animals per cage under standard laboratory conditions, with light on from 0700 to 1900 hours with food and water provided *ad libitum*. Behavioral testing started at an age of 3–4 months. Animals were tested in a randomized manner, alternating tgDISC1 rats and NCs, without blinding.

If not stated otherwise, then the behavioral experiments were conducted in a separate sound-attenuated room and experiments were performed under dim light. Behavior was recorded using an Eyseo Ecoline Standard TV7002 camera (ABUS, Wetter, Germany) and analyzed with the EthoVision software (EthoVision 3.1; Noldus, Wageningen, The Netherlands). After each trial in each experiment arena and objects were cleaned with 70% ethanol. An $n = 12$ was used for all behavioral analyses if not otherwise stated.

A routine pathology survey using conventional methods, for example, hematoxilin–eosin and cresyl violet staining, did not show any aberrant changes in organs of the central nervous system (brain, myelon), peripheral nervous system (nervus ischiadicus), endocrinum (pituitary gland, thyroid glands and adrenal glands), as well as in peripheral organs (lung, liver, kidney, spleen, pancreas, gut, heart muscle and lymph nodes) upon a routine exam (data not shown).

Novelty preference tasks. The tasks were carried out in an open-field arena (60 × 60 × 30 cm, l × w × h) with cues for orientation. Object exploration was recorded manually, the criterion for exploration being active examination of the presented objects. Two 1.5-l plastic water bottles, one filled with clear water, the other one with purple-colored solution, were used as objects. The day before the novelty preference tests animals were allowed to habituate to the arena for 10 min without presentation of objects. Tests were separated by one week to minimize memory interference between the tasks. Animals that did not explore an object in either sample or test trial were excluded from the analysis (object recognition (OR): NC $n = 2$ animals excluded; object place recognition (OPR): NC $n = 4$ animals excluded).

Object recognition. Animals were allowed to explore the arena with two identical objects for a 5-min sample trial, followed by a second 5-min test trial separated by a 25-min intertrial interval. In the test phase one object was replaced by a new one, keeping the original positions. OR is defined as increased exploration of the novel in contrast to the old object.

Object place recognition. This test consists of a 5-min sample trial with two similar objects, a 25-min intertrial interval and a 5-min test trial. In the test trial animals are presented with one object at the same position as in the sample trial (stationary object) and one displaced object that has been moved to a new location. OPR is defined as increased exploration of the displaced compared with the stationary object.

Rotarod. For the testing of motor learning, animals were trained to walk on the rotating cylinder of a rotarod apparatus (Accelerating Rota-Rod, Jones & Roberts, for rats 7750, Ugo Basile, Gemonio, Italy). Three trials with a constant pace of 1 r.p.m. separated by a 50-min intertrial interval were performed. In the first trial each animal had 120 s to learn the task and was supported by the experimenter to keep balance until it learned to walk on the wheel for 3 s on its own. In the following trials animals were left alone once they kept balance. Animals that failed to learn to walk on the wheel in the following trials were excluded from the analysis (NC $n=2$, TG $n=1$). The trial was ended when the animal fell off the rotarod. The latency to fall in seconds was measured manually.

Low-dose amphetamine challenge. Testing was carried out in the TruScan open-fields (Coulbourn Instruments, Whitehall, PA, USA), located in sound- and light-isolated chambers ($110\times70\times70$ cm) on two consecutive days for 15 min each. On the first day the rats were tested following an injection of saline (1 ml kg^{-1}; intraperitonial (i.p.)), on the second day their behavior was recorded following the administration of d-amphetamine (0.5 mg kg^{-1}; i.p.; in saline with an injection volume of 1 ml kg^{-1}; Sigma-Aldrich, St. Louis, MO, USA). Locomotion was automatically measured by the TruScan light beam system.

Generation of mice with increased DAT and decreased VMAT2 expression

DAT overexpressing (DAT-OE) mice were generated using BAC transgenesis as previously described.[31,32] In addition, mice with decreased VMAT2 expression (VMAT2-DE) were generated by gene targeting as outlined elsewhere.[33,34] DAT-OE and VMAT2-DE mice were inter-crossed to produce double-transgenic mice (DAT-OE:VMAT2-DE) that simultaneously display high DAT expression and low VMAT2 expression (Masoud and Ramsey, unpublished). DAT-OE:VMAT2-DE mice were used to model accumulation of cytosolic dopamine due to increased dopamine uptake coupled with reduced vesicular storage. All mice have a C57BL/6 background.

Synaptic plasma membrane preparation and DAT levels

Synaptic plasma membrane fractions of the striatum were prepared as previously described.[35,36] Striata were removed from the fresh rat brains, frozen in 2-methylbutane on dry ice and stored at −80 °C until used.

Measurement of D2High

The method for measuring the dopamine D2High receptors in rat striata *in vitro* was performed as reported earlier.[37,38] Striata were removed from the fresh rat brains and stored at −80 °C until usage. The dopamine receptors in the rat striatal tissue were measured with [^{3}H]domperidone (2 nM final concentration; custom synthesized as [phenyl-^{3}H (*N*)]domperidone; 41.4 Ci per mmol; made by Moravek Biochemicals and Radiochemicals, Brea, CA, USA).

Dopamine D2High receptors were best defined by the number of D2 receptors occupied by 100 nM dopamine, as compared with 1 nM dopamine (where dopamine does not occupy any significant amount of D2 receptors; see ref. 38). Therefore, D2High was measured by the amount of [^{3}H]domperidone bound at 1 nM dopamine minus the amount bound at 100 nM dopamine (Y). The specific binding, S, of [^{3}H]domperidone at 2 nM was measured by the amount of [^{3}H]domperidone bound at 1 nM dopamine minus the amount bound in the presence of 10 μM *S*-(-) sulpiride. The percent of D2 receptors in the high-affinity state was defined by $(Y/S)\times100\%$.

Cyclic voltammetry

Rats were sacrificed by rapid decapitation. The head was immediately submerged into oxygenated ice-cold sucrose buffer. Following removal of the brain, coronal slices (350 μm) from NC and TG animals were sectioned with a vibratome and incubated at 32 °C in artificial cerebrospinal fluid (aCSF). DA release was electrically stimulated (1 pulse, 350 μA) using a double-pronged stainless steel stimulating electrode placed into the region of interest. DA release was recorded using a carbon fiber microelectrode, placed in the slice to form an equilateral triangle with the stimulating electrode. A cyclic voltage ramp (−0.4 V to 1.0 V to −0.4 V) was applied to the carbon fiber microelectrode and the resultant background-subtracted current was measured. Application of waveform, stimulus and current monitoring was controlled by TarHeel CV (University of North Carolina), using a custom potentiostat (UEI, UNC Electronics Shop). A 5-stimulation recording survey of four different dorsal striatal and nucleus accumbens sites were taken for each animal with a 5-min rest interval between each synaptic stimulation. Following the experiment, the carbon fiber microelectrode was calibrated using a flow-cell injection system and known dopamine standards. Kinetic constants were extracted using nonlinear regression analysis of release and uptake of dopamine from the extracellular space.

Receptor autoradiography

Animals were decapitated and their brains rapidly removed and immediately frozen in 2-methylbutane (−50 °C) and stored until sectioning. Coronal sections (20 μm) were produced in a cryostat microtome (Leica, Nussloch, Germany), thaw-mounted onto silica-coated object slides and stored at −80 °C until further use.

Dopamine D2 receptors were labeled accordingly with [^{3}H]raclopride (0.56 nM) in 50 mM Tris-HCl (pH 7.4; 45 min at 22 °C) containing 0.1% ascorbic acid and NaCl (150 mM), using the displacer butaclamol (1 μM).

Slices exposed to phosphor-imaging plates for 3 days together with tritium standards. Autoradiograms from phosphor-imaging plates were scanned with a high-performance plate reader and subsequently processed in a blinded manner using image-analysis software (AIDA 4.13; all Raytest, Straubenhardt, Germany).

Neurochemical analysis of *post-mortem* brain tissue

After dissection brain tissues were homogenized with an ultrasonic device in 0.05 M perchloric acid (Janssen, Geel, Belgium) containing deoxyepinephrinehydrochlorid (Sigma-Aldrich) as the internal standard. Dopamine content was electrochemically detected as previously described[39] and analyzed with the Chrom Perfect Software (Justice Laboratory Software, Denville, NJ, USA).

Rat and mouse insoluble proteome preparation

Transgenic and control mouse brain medial prefrontal cortex (mPFC) and hemispheres of heterozygous TG and NC rats were isolated and weighed. Each tissue piece was homogenized in 2.5% buffer A (50 mM HEPES pH 7.5, 300 mM NaCl, 250 mM sucrose, 5 mM GSH, 5 mM $MgCl_2$, 1% NP-40, 0.2% sarcosyl, 2× protease inhibitor, 1 mM PMSF), supplemented with 40 U ml^{-1} DNaseI and incubated for 30 min at 37 °C followed by 16 h at 4 °C.

Next, samples were spun at $1800\times g$ for 30 min at 4 °C. The pellet was resuspended in buffer B (50 mM HEPES pH 7.5, 1.5 M NaCl, 250 mM sucrose, 5 mM EDTA, 5 mM GSH, 1% NP-40, 0.2% sarcosyl, 2× protease inhibitor, 1 mM PMSF) and centrifuged at $1800\times g$ for 30 min at 4 °C. The resulting pellet was washed in buffer C (50 mM Tris pH 8, 250 mM sucrose, 5 mM GSH, 1% NP-40) and spun at $1800\times g$ for 30 min at 4 °C. The pellet was resuspended in buffer D (50 mM HEPES pH 7.5, 5 mM GSH, 1% NP-40, 2× protease inhibitor). Finally, the pellet was resuspended in buffer D′ (50 mM HEPES pH 7.5, 0.2% sarcosyl, 2× protease inhibitor) and spun at 100 000 x *g* for 45 min at 4 °C in an ultracentrifuge (TLA-55 rotor in Optima; Beckman Coulter, Krefeld, Germany). The resulting insoluble pellets were solubilized in 2× SDS-loading buffer and used for western blots. Thus, we define insoluble pellet as what is pelleting after centrifugation in cold ionic detergent.

The preparation of the insoluble proteome of mPFC and dStr of transgenic rats was performed as previously described.[20] Transgenic DISC1 was detected with the huDISC1 specific mAb 14F2 and fluorescent secondary anti-mouse antibody (IRDye 800CW Goat anti-Mouse IgG, LI-COR Biosciences, Lincoln, NE, USA).

Structural MRI analysis and calculation of ventricle size

Structural MRI imaging was performed on a 7.0 tesla small animal Scanner (Bruker BioSpin, Billerica, MA, USA) with a horizontal bore magnet. The system included a 20-cm Gradient and a 29-cm shimm system. For RF transmission a transmit only quadrature coil (inner diameter 86 mm) (Bruker BioSpin) was used. RF reception was carried out with a rat brain 20-mm surface loop coil (Bruker BioSpin). Forty-eight coronal slices ($0.156\times0.156\times0.5$ mm) with a matrix of 256×256, FOV 4 cm × 4 cm, were recorded using a RARE sequence: TE 14.370 ms, TR 7080 864 ms, 4 averages, RARE factor of 4, scan duration of 15 min 6 s. During image recording animals were kept under 2% isoflurane. Respiration and body temperature were monitored and controlled throughout the entire

experiment. For the analysis the Anatomist/ BrainVisa program version 4.3.0 (NeuroSpin, Gif-sur-Yvette, France) was used.

Immunohistochemistry of rat brains

For the immunostaining of transgenic rats animals were perfused with phosphate-buffered saline (PBS) pH 7.4 and sagittal cryo sections were cut on a Cryostat (Leica CM1900; Leica, Germany) and dried for 20 min at RT. The sections were post-fixed with ice-cold 4% paraformaldehyde solution buffered with PBS pH 7.4 (PFA, Sigma-Aldrich, MO, USA). After blocking with antibody diluent (Dako, Hamburg, Germany) sections were incubated with the mAb 3D4 for 16 h at 4 °C in antibody diluent. After two PBS washes the secondary antibody (anti-mouse IgG AlexaFluor594 1:300; Invitrogen) was applied for 1 h at RT. Sections were washed in PBS and in PBS plus 0.05% Tween-20 for 10 min. Subsequently sections were washed shortly in distilled water, 70% ethanol and incubated 2× 5 min in Sudan Black (Division Chroma, Münster, Germany) in 70% ethanol to block autofluorescence. After washing the sections in 70% ethanol and H_2O, they were mounted with ProLong Gold containing DAPI (Invitrogen). All images were collected with a Zeiss Axiovision Apotome.2 confocal microscope (Zeiss, Oberkochen, Germany).

Dopamine-induced DISC1 insolubility in cell culture

Human neuroblastoma SH-SY5Y cells were obtained mycoplasma-free from the DSMZ (Leibniz Institute DSMZ-German Collection of Microorganisms and Cell Cultures, Braunschweig, Germany) and tested at irregular time intervals for mycoplasma contamination. SH-SY5Y cells expressing inducible full-length human DISC1 were generated using the Retro-X Tet-On Advanced Inducible Expression System (Clontech Laboratories, Mountain View, CA, USA). SH-SY5Y cells were seeded onto glass coverslips, induced for 24 h, treated with 100 μM DA for 24 h and fixed with 4% PFA in PBS. Cells were permeabilized with PBS (plus 0.5% saponine, 5% milk powder, 1% BSA) and incubated with the mAb 14F2 and/or a vimentin antibody (1:100; Cell Signaling, Danvers, MA, USA) and subsequent AlexaFluor594 secondary antibody (Invitrogen) for 1 h in PBS plus 0.5% saponine and 1% BSA was used. Cells were mounted with ProLong Gold with DAPI (Invitrogen). Images were collected with a Zeiss Axiovision Apotome.2 confocal microscope (Zeiss).

Purification of the insoluble proteome of human neuroblastoma (NLF) cells transfected with DISC1 and primary cortical neurons of the tgDISC1 rats were performed as described previously.[6] Primary neurons at DIV 14 were incubated with 50 μM DA for 24 h to induce DISC1 aggregation and then underwent the insoluble proteome purification.

Cryoimmunogold electron microscopy

Cryoimmunogold electron microscopy was performed as described previously.[40]

Co-immunoprecipitation of DISC1 by DAT in striatal membrane preparations and cell lysates

For the co-immunoprecipitation (co-IP) of DAT and DISC1 striata of adult tgDISC1 rats were dissected and the plasma membrane fraction was purified by a sucrose gradient. The striatal tissue was homogenized in buffer A (250 mM sucrose, 50 mM HEPES pH 7.4, 15 mM EDTA pH 8, 3 mM DTT, protease inhibitor). After centrifugation at 500 × *g* for 5 min at 4 °C 1 ml of the supernatant was mixed with 1.7 ml of buffer D (2 M sucrose, 50 mM HEPES pH 7.4, 15 mM EDTA pH 8, 3 mM DTT, protease inhibitor) to gain a final sucrose concentration of 1.34 M (now solution C). The sample was layered on top of 1 ml of buffer D, followed by 1 ml of buffer B (850 mM sucrose, 50 mM HEPES pH 7.4, 15 mM EDTA pH 8, 3 mM DTT, protease inhibitor) and buffer A in 5 ml ultracentrifugation tubes (Beckman Coulter, Krefeld, Germany). The samples were centrifuged for 16 h at 100 000 × *g* at 4 °C (MLS-50 rotor in Optima; Beckman Coulter, Germany). Afterwards the interphase between layer B and C containing the membrane fraction was collected, diluted with 3 volumes of PBS and frozen at − 80 °C for 2 h for precipitation. After thawing and pelleting by centrifugation (14 000 × *g* at 4 °C for 30 min), the membrane fractions were resuspended in RIPA buffer (50 mM Tris pH 7.6, 150 mM NaCl, 1% NP-40, 0.5% DOC, 0.1% SDS, supplemented with 0.5 mM DTT and protease inhibitor).

For the co-IP the solubilized membrane fractions (input: one rat striatal hemisphere per IP reaction) were equally divided. One sample did not receive an antibody for capturing, the other one was mixed with 3 μg of a polyclonal antibody raised against DAT (AB2231, Merck Millipore, Darmstadt, Germany) and incubated for 2 h at 4 °C, before addition of 20 μl of Protein A/G magnetic beads (Pierce, Rockford, IL, USA) and further incubation for 16 h at 4 °C. The beads were washed 4× with 1 ml of 50 mM Tris pH 7.6, 150 mM NaCl, 0.05% NP-40 and precipitated proteins were eluted by addition of loading buffer containing 2% β-mercaptoethanol for 10 min without boiling. Subsequently, the samples were used for western blot and membranes were incubated with the 14F2 (detecting huDISC1) and MAB369 antibody (detecting DAT; Merck Millipore).

Primary antibodies

For western blot: actin (rabbit, 1:10 000; Sigma-Aldrich); DAT (rat MAB369, 1:1 000; Merck Millipore); huDISC1 (mouse 14F2, 1:1 000; Korth lab[21]); ratDISC1 (rabbit hu-precleared C-term,1:1 000; Korth Lab[41]); Na/K-ATPase (rabbit, 1:1500; Cell Signaling; the antibody detects the α1 subunit. On the basis of sequence homology, the antibody could also cross-react with α2 and α3 isoforms); Tubulin (mouse, 1:10 000, Sigma-Aldrich). For immunostaining: human DISC1 for ICC (mouse 14F2, 1:250; Korth lab); human DISC1 for IHC (mouse 3D4, 10 μg ml^{-1}; Korth lab[20]); Vimentin for ICC (rabbit D21H3, 1:100; Cell Signaling).

Western blot

For western Blots the Novex NuPAGE SDS-PAGE Gel System (all: Thermo Fisher Scientific) with the corresponding NuPAGE Novex 4–12% Bis-Tris Midi Protein Gels, NuPAGE MES SDS Running buffer and NuPAGE LDS Sample Buffer (4×, plus 8% β-mercaptoethanol) or Laemmli loading buffer (4×, 200 mM Tris pH 6.8, 40% glycerol, 10% SDS, 0.4% bromphenolblue, 8% beta-mercaptoethanol) was used. For molecular size estimation the PageRuler Prestained Protein Ladder (#26617; Thermo Scientific, MA, USA) was used. As the dyes used for prestaining of the marker proteins influence their electrophoretic mobility, the apparent marker size was calibrated to the PageRuler Unstained Protein Ladder (#26614; Thermo Scientific) according to manufacturer's instructions in the gel system used. Accordingly, all depicted marker sizes have subsequently been adapted to the calibrated sizes.

Densitometric analyses

Band intensities were calculated from luminescent sensitive film (Amersham Hyperfilm ECL; GE Healthcare, Buckinghamshire, UK) using the ImageJ 10.2 software (National Institute of Health, Bethesda, MD, USA). Alternatively fluorescent secondary antibodies (LI-COR Biosciences, Lincoln, NE, USA; 1:15 000 in PBS plus 0.05% Tween-20) were used and intensities were analyzed on a LI-COR Odyssey CLX and the corresponding Image Studio Version 2.1 software (LI-COR Biosciences).

Statistics

All statistical analyses were performed as indicated using the IBM SPSS Statistic program (Versions 20–22; IBM, Ehningen, Germany) or GraphPad Prism (Versions 4 and 5; GraphPad Software Inc., San Diego, CA, USA).

All data sets were tested for normal distribution based on the expected experimental results and appropriate parametric or non-parametric tests were chosen. An estimate of variation was made for selected analyses. Comparison of two groups with similar variances was done by Student's *t*-test or Wilcoxon non-parametric test. Analyses were two-sided, if not stated otherwise.

Sample size was chosen according to Fisher's exact test and the expected difference between experimental conditions. Animal behavior was analyzed by two-way repeated measures analysis of variances (ANOVAs) with the variables genotype and treatment, object, or trial, thus considering correcting for multiple testing. Significant effects of the independent variables were explored further by splitting the data appropriately and conduction of lower level ANOVAs and *post hoc* comparisons including respective corrections for multiple testing. Paired sample *t*-tests were applied when appropriate.

Appropriate statistical tests and *P*-values are stated in the respective figure legends and/or results section. *P*-values of $^{*}P \leqslant 0.05$, $^{**}P \leqslant 0.01$, $^{***}P \leqslant 0.001$ were used as significance levels.

RESULTS

Neuropathology of tgDISC1 rats

Previously, we reported the presence of insoluble DISC1 in biochemically purified fractions from *post mortem* cases of the Stanley Medical Research Institute Consortium Collection (SMRI CC)[42] diagnosed with mental illness.[20,21] To model DISC1 aggregation *in vivo*, we generated a transgenic rat modestly overexpressing non-mutant, full-length human DISC1 under control of the Syrian hamster prion protein (PrP) promoter (tgDISC1 rat). These rats showed about 11-fold higher transgenic human DISC1 expression compared with endogenous rat Disc1 protein levels (Supplementary Figure S1a and c; protein expression rates were measured at P58). We chose to include common variants C704 and F607 as they are frequent in the normal population[43] and have been demonstrated to increase the risk to mental illness[4] and, in biophysical studies, DISC1 misassembly.[6,7] The PrP promoter was utilized for two reasons: first, it provides pan-cellular expression in the brain that has previously been demonstrated for DISC1[44] and, second, it leads to sufficient expression levels for inducing misassembly as successfully demonstrated in non-prion animal models of protein conformational disease.[45,46] The PrP promoter is broadly active at embryonic day E13.5 in the mouse brain[47] and continues to be expressed into adulthood, while the *Disc1* gene has two expression peaks at E13.5 and around postnatal day P35.[48]

Four different founder lines were generated (Figure 1a), and the founder line with the lowest expression level was selected (Founder line #3; Figure 1a and Supplementary Figure S2) in order to avoid artifacts due to strong overexpression. The level of overexpression was estimated to be 11-fold higher than endogenous Disc1 protein (Supplementary Figure S1a, c), however, precise determination is impossible due to dozens of splice forms of both endogenous rodent and human DISC1.[49] The chosen founder line exhibited neuronal, mainly perinuclear DISC1 aggregates throughout the brain and in primary neuron preparations that co-stained with the centrosome marker γ-tubulin (Figure 1b, Supplementary Figure S3a, b). We define DISC1 aggregation or misassembly (a broader term) using the following criteria: (1) insolubility in ionic detergents upon biochemical fractionation;[20] and (2) presence of (perinuclear) inclusion-like structures that may represent cellular accumulation of insoluble material, as observed in some protein conformational diseases like, for example, Huntington's disease.

There was accentuated DISC1 aggregation in dopamine-rich dorsal striatum (dStr; Figures 1b and c) that could not be explained by differences in PrP promoter activity (Supplementary Figure S2b), suggesting that posttranslational mechanisms led to an enrichment of aggregated DISC1. Aggregation of the transgenic DISC1 protein also led to recruitment of endogenous rat Disc1 in the insoluble fraction (Supplementary Figures S2c, d).

No major pathology was observed in peripheral organs or the brain of tgDISC1 rats (data not shown). However, we did detect slightly enlarged ventricles in the brain (Figure 1d), a trait also observed in patients with schizophrenia[50] and some transgenic mouse models expressing mutant DISC1.[10,12,13,26] Of note, the mainly perinuclear DISC1 aggregates were not positive for ThS (Supplementary Figure S4a and b), a marker for amyloid, even though a recombinant DISC1 fragment (598–785 (ref. 6)) injected into the brain of wild-type rats did stain for ThS (Supplementary Figure S4c). This indicates that DISC1 or its fragments are principally able to form amyloid, but not when endogenously expressed in adult or aged tgDISC1 rats.

Dopamine-related behavioral phenotypes of tgDISC1 rats

Similar to patients with schizophrenia,[51] tgDISC1 rats exhibited spontaneous amphetamine supersensitivity. When challenged with a single low-dose of 0.5 mg kg^{-1} d-amphetamine (Figures 2a and b), tgDISC1 rats exhibited increased locomotion and rearing behavior, whereas negative control rats did not. A two-way ANOVA revealed a main effect for treatment (distance: $F_{1,22} = 19.026$, $P < 0.001$; rearing: $F_{1,22} = 43.909$, $P < 0.001$) and genotype-treatment interaction (distance: $F_{1,22} = 6.052$, $P = 0.022$; rearing: $F_{1,22} = 17.706$, $P < 0.001$). A paired *t*-test of locomotion data during saline and amphetamine for the two genotypes revealed that tgDISC1 rats exhibited a large increase in locomotion upon amphetamine treatment (distance and rearing: $P < 0.001$), whereas NCs did not respond (distance: $P = 0.280$; rearing $P = 0.146$). Amphetamine supersensitivity was persistent even in 22-month-old tgDISC1 animals (Supplementary Figures S5a and b). This suggests that disturbance in the dopamine system of tgDISC1 rats is a persistent, life-long trait.

Furthermore, tgDISC1 rats exhibited motor deficits in the rotarod task (Figure 2c). A two-way ANOVA checking for genotype differences in the learning curve of the rotarod task showed a main effect for genotype ($F_{1,19} = 7.534$, $P = 0.013$) and trial ($F_{2,38} = 3.360$, $P = 0.045$). Subsequent *post hoc* unpaired *t*-tests for trials 1, 2, 3 comparing genotypes revealed a significant difference in trial 3 performance ($P = 0.041$), whereas no differences could be detected in the first two trials (trial 1: $P = 0.217$; trial 2: $P = 0.122$). These major behavioral phenotypes were confirmed in a different founder line as well (Supplementary Figure S6).

Spatial and object memory was also tested in tgDISC1 rats using novelty preference tasks. Although both genotypes could distinguish objects in the OR, OPR and object recognition for temporal order paradigms (Supplementary Figure S7), tgDISC1 rats displayed a marked preference towards novel objects compared with controls (Figures 2d and e). This preference was also persistent in old age (Supplementary Figures S5c and d). In the OR task, rats have to identify the new object presented in the test trial. A two-way ANOVA showed main effects for object ($F_{1,20} = 31.110$, $P < 0.001$) and object-genotype interaction ($F_{1,20} = 9.343$, $P = 0.006$). A subsequent one-way ANOVA revealed genotype differences in hyperexploration of the new, but not the old object (old $P = 0.737$, new $P = 0.048$). However, in general both genotypes preferred exploration of the new over the old object (data split for genotype; paired *t*-test: NC $P = 0.045$, TG $P < 0.001$). Comparable behavioral results were detected in the object place recognition task in which the animal has to discriminate between the displaced and the stationary object. Here, the two-way ANOVA showed main effects for both object ($F_{1,18} = 26.118$, $P < 0.001$) and genotype ($F_{1,18} = 6.923$, $P = 0.017$), again highlighting hyperexploration of the more interesting displaced object in tgDISC1 rats (one-way ANOVA stationary $P = 0.128$, displaced $P = 0.019$). Comparisons of exploration time of the stationary and displaced object by a paired *t*-test show that both genotypes investigate the displaced object for longer (NC $P = 0.021$, TG $P = 0.001$).

As amphetamine supersensitivity indicated a disturbance in the dopaminergic system, we performed *ex vivo* neurochemistry and analysis of dopamine receptor densities in the striatum of tgDISC1 rats. Dopamine concentrations were decreased in the dStr (Figure 3a), amygdala and hippocampus (Supplementary Figures S8a and b) of tgDISC1 rats. However, no changes were detected in total D2Rs (Figure 3b), D1 receptors (D1Rs), serotonergic, or glutamatergic receptors (Supplementary Figure S8c) as measured by receptor autoradiography. Surprisingly, when we investigated the affinity state of D2Rs, we found an ~80% increase in high affinity D2 (D2High) receptors in tgDISC1 rats (Figure 3c). A switch from low-affinity D2Low to D2High receptors is a characteristic feature of schizophrenia.[52,53] To investigate whether the changes in D2R affinity state affected signaling in striatal medium spiny neurons (MSNs), we assessed substance P and enkephalin expression as markers of neuronal activity

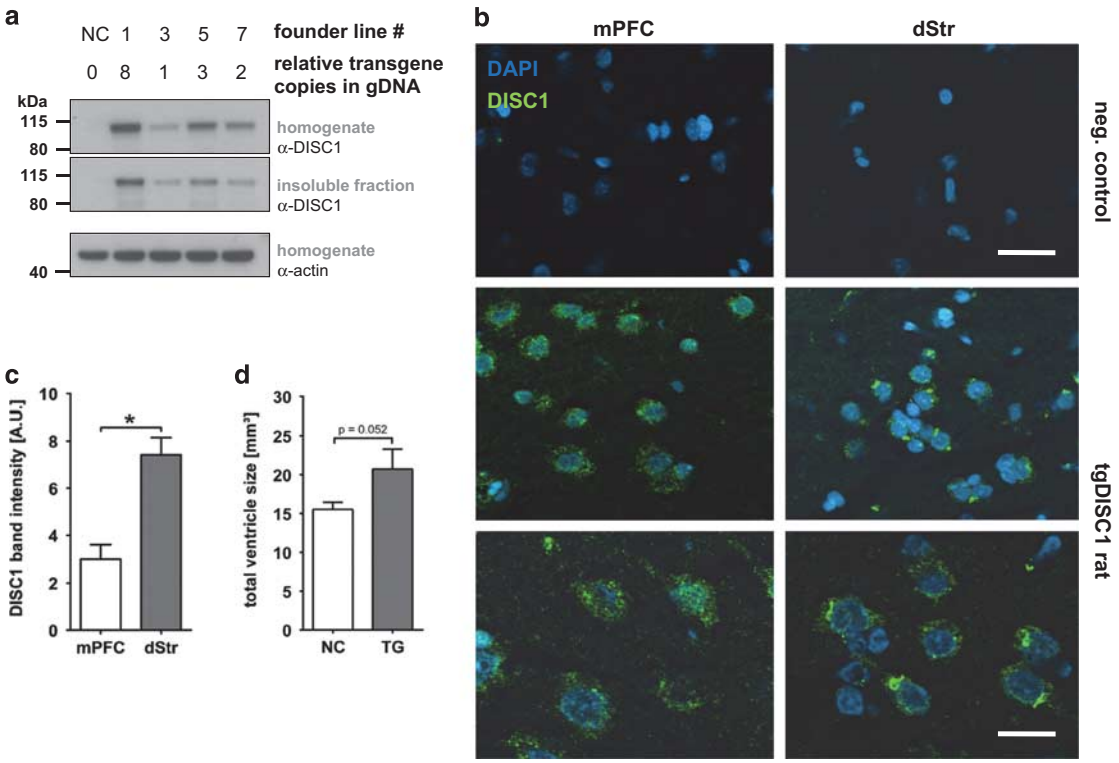

Figure 1. Aggregated DISC1 detected by IHC in brains of the tgDISC1 rat. (**a**) Western blot comparing transgene expression and aggregation in four different tgDISC1 founder lines. Heterozygous rats of founder lines 1, 3, 5 and 7 displayed different levels of full-length human DISC1 transgene expression (homogenate) which were reflected in the insoluble fraction. No huDISC1 could be detected in the negative control animal. Beta-actin was used as loading control in the homogenate. Relative number of transgene copies in founder lines was determined by quantitative Real-Time-PCR of genomic DNA and revealed the least transgene copies in the gDNA of founder 3 (arbitrarily set to one for comparison between founder lines) and a Mendelian-like inheritance pattern upon breeding. Founder line 3 with the weakest DISC1 expression was chosen for further experiments to avoid artifacts of too strong transgene expression. (**b**) Confocal immunofluorescence of striatal (dStr, right panels) and frontal (left panels) cryosections of the transgenic DISC1 rat (middle and in higher magnification in lower panels) and a negative control rat (upper panels). Abundant punctuate, mainly perinuclear staining as evidence for the existence of DISC1 aggregates can be detected that are more frequent and bigger in the striatum. Green: DISC1; blue: DAPI; bar 40 μm (upper two panels), bar 10 μm (lower panels). (**c**) Densitometric analysis of biochemically purified insoluble fraction of the tgDISC1 rat mPFC and dorsal striatum. The tgDISC1 rat ($n = 6$) had more aggregated DISC1 in the dStr than in the mPFC in accordance with the IHC. Wilcoxon $^*P = 0.028$. (**d**) NMR analysis of ventricle size. The tgDISC1 rat ($n = 8$) had a larger total ventricle size than negative controls ($n = 10$), namely 20.75 ± 2.5 mm^3 in tgDISC1 rats and 15.54 ± 0.9 mm^3 in negative controls. Unpaired *t*-test: $P = 0.052$. All means ± s.e.m. DISC1, Disrupted-in-Schizophrenia 1; gDNA, genomic DNA; NMR, nuclear magnetic resonance.

in D1R- and D2R-expressing MSNs (Supplementary Figure S8d), respectively. We did not find significant changes indicating that altered dopamine transmission in the dStr was not strong enough to induce changes in substance P or enkephalin expression.

To further characterize the dopaminergic system, we performed fast-scan cyclic voltammetry in striatal slices from tgDISC1 rats and controls. Peak dopamine release was similar between genotypes (Figure 3d) but, interestingly, extracellular dopamine clearance was increased in the dStr of tgDISC1 rats (Figure 3e, see also Supplementary Figure S8e), indicating elevated DAT function. Therefore, using dissected striata, we further investigated the cellular localization of DAT. In tgDISC1 rats, significantly more DAT was translocated to the plasma membrane, likely explaining the observed increase in dopamine clearance (Figure 3f and Supplementary Figure S8f).

Taken together, these findings indicate that dopamine homeostasis is changed in tgDISC1 rats, as evidenced by D2R affinity state and DAT function. Thus, misassembly of full-length human DISC1 is sufficient to cause changes in the dopaminergic system consistent with some biochemical and behavioral symptoms seen in schizophrenia or psychosis.

Molecular and cellular interactions between DISC1 protein assembly and the dopamine system

To further investigate interactions between DISC1 assembly and dopamine on the cellular and molecular level, we generated full-length human DISC1-inducible SH-SY5Y cell lines (Figure 4a). We did not detect different aggresomal sizes in the cell lines expressing either the full-length human DISC1 (S704, L607) or the (C704, F607) variant (Supplementary Figure S9). This suggests that changes in misassembly of DISC1 polymorphisms observed in biophysical studies do not translate to microscopically visible differences. When these cells were induced to drive DISC1 expression and then exposed to a high, but non-toxic concentration of dopamine for 24 h, DISC1 aggresomes were detected (Figures 4a and c; Supplementary Figure S10a). The DISC1 aggresomes were coated with vimentin, a defining marker for aggresomes[54] (Figure 4c, Supplementary Figures S9a and b), which also makes it unlikely that DISC1 is a component of the aggresome machinery itself. Primary neurons and brain slices of the tgDISC1 rat could not be stained to check for vimentin coating of aggresomes, as vimentin is only expressed in proliferating tissues.[55] However, these cellular perinuclear DISC1 aggresomes co-localized with γ-tubulin, but neither with HSP70, nor the

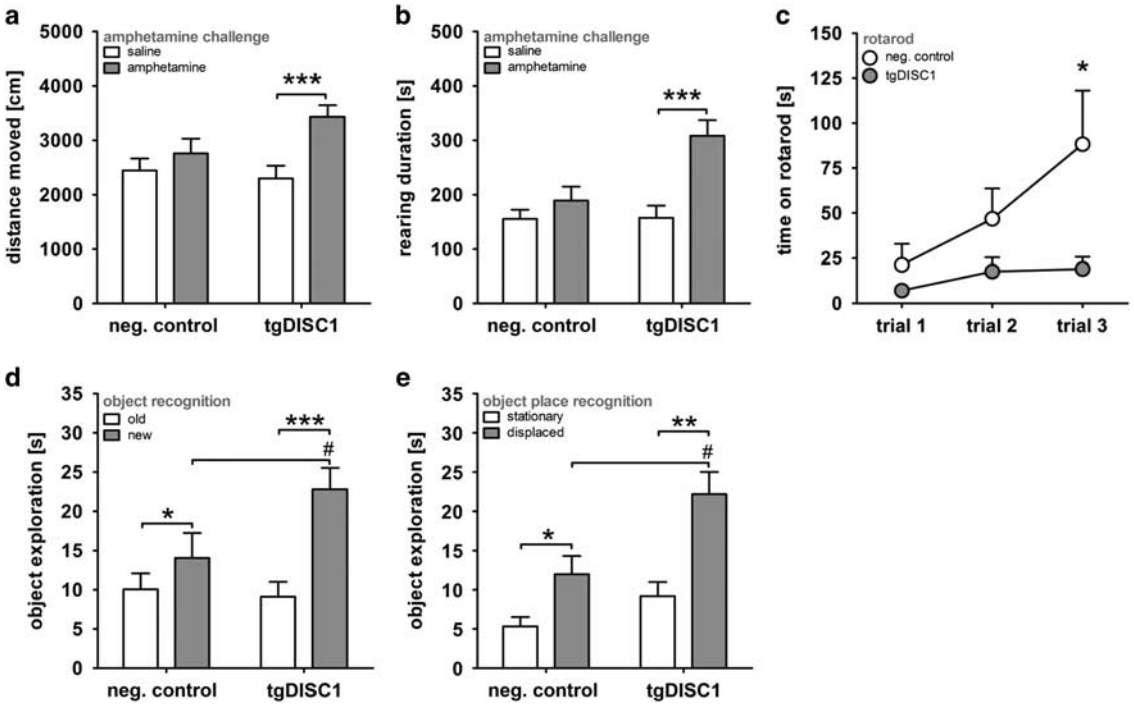

Figure 2. Behavioral phenotypes of the tgDISC1 rat. (**a**) Amphetamine hypersensitivity in the tgDISC1 rat shown by horizontal locomotion. Spontaneous locomotion before (saline; white bars) and after (gray bars) application of a single low dose of d-amphetamine (0.5 mg kg^{-1}, i.p.) is presented. Whereas the d-amphetamine had no significant locomotor effect in the control animals (paired *t*-test: $P = 0.280$, $n = 12$), it led to increased locomotion in the tgDISC1 rat indicating hypersensitivity to d-amphetamine (paired *t*-test $^{***}P < 0.001$, $n = 12$). (**b**) Amphetamine hypersensitivity in the tgDISC1 rat shown by duration of rearing. Only tgDISC1 rats reacted with increased duration of rearing to d-amphetamine treatment (gray bars) compared with saline (white bars; paired *t*-test: negative controls (NC) $P = 0.146$, TG $^{***}P < 0.001$; TG and NC $n = 12$). (**c**) The rotarod task as measure of motor learning ability and attention. Under constant speed of the wheel, the negative control animals showed a significant progressive improvement in walking on the rotarod over three subsequent trials, whereas the transgenics did not display such a learning curve (*t*-test of trial 3: $^{*}P = 0.041$; TG $n = 11$, NC $n = 10$). (**d**) Hyperexploration of tgDISC1 rats in the object recognition task (OR). Comparing duration of exploration of the new vs the old object in tgDISC1 rats and controls during OR test trial (TG $n = 12$, NC: $n = 10$) showed that tgDISC1 rats explored the new object more extensively than the negative controls (one-way ANOVA: $^{\#}P = 0.048$), although both genotypes preferred the new over the old one (paired *t*-test: NC $^{*}P = 0.045$, TG $^{***}P < 0.001$). (**e**) Hyperexploration of the tgDISC1 rats in the object place recognition task (OPR). Comparably, in the OPR task (TG $n = 12$, NC $n = 8$) the tgDISC1 rats explored the displaced object longer than control rats (one-way ANOVA: $^{\#}P = 0.019$). Again, both genotypes favored the displaced over the stationary object (paired *t*-test; NC $^{*}P = 0.021$, TG $^{**}P = 0.001$). All means ± s.e.m. DISC1, Disrupted-in-Schizophrenia 1; i.p., intraperitonial.

oligomer-specific marker A11, or the amyloid marker ThT (Supplementary Figure S10b and c).

This increase in DISC1 misassembly upon exposure to dopamine is consistent with our observation of increased DISC1 aggregation in the dStr (Figures 1b and c), which is the brain region with the highest dopamine content (Supplementary Figure S8b).

These results suggest a bidirectional link between dopamine homeostasis and DISC1 assembly because not only did DISC1 assembly regulate D2R affinity state and DAT function *in vivo,* but also because increased cytosolic dopamine itself augmented DISC1 insolubility. To investigate whether DISC1 could interact in a complex with DAT we performed co-immunoprecipitation experiments. First, using plasma membrane fractions from the striatum of tgDISC1 rats, we demonstrated that DAT antibody co-immunoprecipitated transgenic human DISC1 (Figure 4d). Second, using SH-SY5Y cells that overexpress DISC1 and DAT, we demonstrated co-immunoprecipitation of DISC1 by DAT (Supplementary Figure S11b), as well as subcellular colocalization *in vivo* of the two proteins using immunofluorescence and the Proximity Ligation Assay[56] (Supplementary Figures S12). Furthermore, dopamine-induced DISC1 aggregates (Figure 4a) were also able to sequester DAT into the insoluble fraction (Supplementary Figures S13c and d). Taken together, all these *in vivo* and *in vitro* results converge on the demonstration of a functional complex comprising DISC1 and DAT.

Pulse treatment of DISC1-transfected cell lines and primary neurons of the tgDISC1 rat with a single, high and non-toxic dose of dopamine induced a high-molecular-weight (HMW) band with an electrophoretic mobility of ~200–230 kDa in western blots suggesting a biochemical signature of dopamine-induced DISC1 multimers (Figure 5a and Supplementary Figure S14a). The identity of this band as DISC1 was confirmed by mass spectrometry (Supplementary Figure S14b and c). Dopamine-induced appearance of this HMW band and aggresome-positive cells could not be prevented by addition of D1R or D2R antagonists (Supplementary Figure S15). However, it was partially inhibited by a DAT inhibitor (Supplementary Figure S16) suggesting that these phenotypes were not induced by signaling events but by the presence of cytosolic dopamine.

To further investigate whether conditions that lead to increased cytosolic DA *in vivo* can also induce the HMW DISC1 band, we used transgenic mice that are postulated to have elevated levels of cytosolic dopamine. In particular, we used mice that either overexpress DAT (DAT-OE), underexpress VMAT2 with only ~5% of normal levels (VMAT2-DE) or double-transgenic mice (DAT-OE: VMAT2-DE). Using purified insoluble fractions from the mPFC of these mice, we demonstrated an increase in the endogenous HMW DISC1 band in DAT-OE and DAT-OE:VMAT2-DE brains (Figure 5b), thus confirming cytosolic dopamine-induced aggregation of DISC1 *in vivo*. The identity of this HMW band

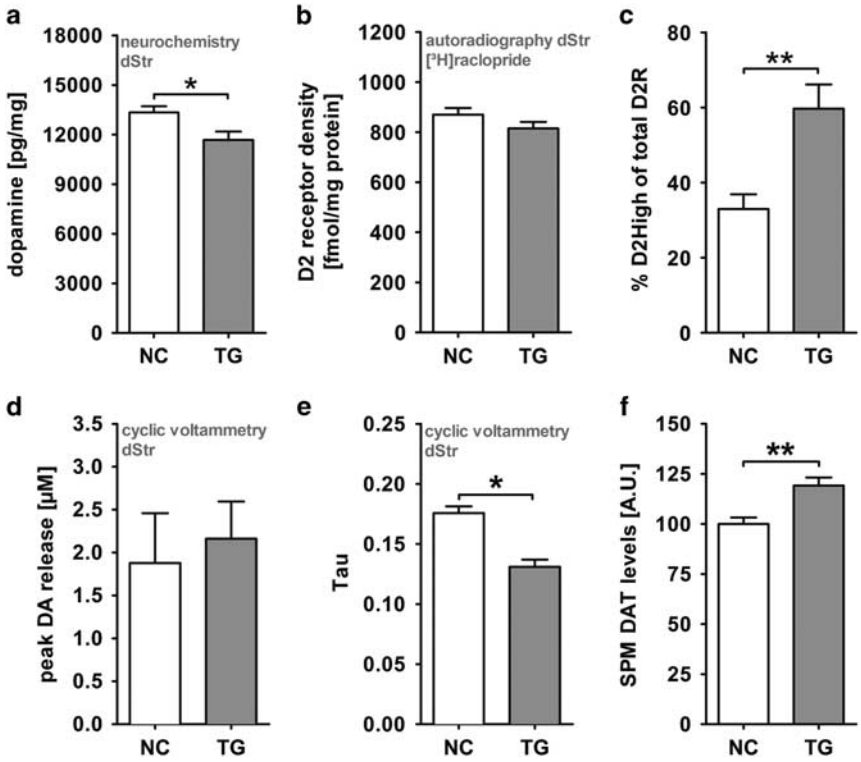

Figure 3. Dorsal striatum and dopamine homeostasis in the tgDISC1 rat. (**a**) Neurochemical quantification of *post mortem* dopamine (DA) in the dStr of tgDISC1 and negative control animals. TgDISC1 rats ($n=12$) had lower levels of DA as compared with negative controls (NCs) ($n=12$). TgDISC1 and negative control rats had 13 337 ± 375 and 11 675 ± 504 pg/mg DA. Unpaired *t*-test $^{**}P=0.005$. (**b**) Total D2 receptor abundance in the dStr. Autoradiography was performed with the D2R specific radioligand [^{3}H]raclopride. No difference in ligand binding and therefore total receptor density could be found in tgDISC1 rats ($n=10$) and controls ($n=10$) in the dorsal striatum. Mean receptor density was 870 ± 26 fmol/mg protein for controls and 815 ± 26 for tgDISC1 rats. Unpaired *t*-test $P=0.156$. (**c**) Elevated striatal D2High receptor portion in tgDISC1 rats. TgDISC1 rats ($n=6$) had an 81% increase in D2High receptor portions compared with negative controls ($n=6$) as measured by [^{3}H]domperidone binding. Binding of the radioligand was challenged with either 1 nM or 100 nM DA, concentrations at which no significant occupation of D2Rs or D2High-specific binding occurs, respectively. Proportions of D2High receptors in relation to total D2 receptors were 33 ± 3.9% in NCs and 59.7 ± 6.5% in TGs. Unpaired *t*-test $^{**}P=0.005$. (**d**) Peak DA release in the dStr of tgDISC1 rats. Fast-scan cyclic voltammetry measurement of DA in striatal slices revealed no difference in the peak release of DA in tgDISC1 rats (2.16 ± 0.43 µM; $n=4$) and controls (1.88 ± 0.58 µM; $n=6$). Mann–Whitney *U*-test $P=0.762$. (**e**) Clearance of extracellular DA in the dStr of tgDISC1 rats. TgDISC1 rats (tau = 0.131 ± 0.006; $n=4$) show increased extracellular DA clearance compared with negative controls (0.176 ± 0.006; $n=6$) as measured by fast-scan cyclic voltammetry. Mann–Whitney *U*-test $^{*}P=0.036$. (**f**) Striatal DAT levels in tgDISC1 rats. Preparation of the synaptic plasma membrane (SPM) and subsequent western blotting revealed a 19% increase in dopamine transporter levels in the dorsal striatum of tgDISC1 rats (NC, TG $n=6$). Densitometric analysis was performed by normalization of DAT to the Na/K-ATPase signal in the preparations. Unpaired *t*-test $^{**}P=0.004$. All means ± s.e.m.

under different conditions was determined for endogenous rat and mouse Disc1 as well as artificially expressed human DISC1 (in tgDISC1 rats) using an overlay of species-specific antibody signals (Figure 5c).

Amphetamine sensitization is a pharmacological model of psychosis.[57] Amphetamine is known to block and even reverse DAT's ability to transport dopamine out of the presynapse,[58] thereby enhancing extracellular dopamine concentrations. Sensitization with amphetamine leads to the depletion of stored dopamine in the striatum and enhancement of dopamine in the typically low dopamine-containing mPFC.[57] We sensitized wild-type rats for 5 days with daily doses of 2 mg kg^{-1} amphetamine, and probed them after a 2-week interval with a single dose of 0.5 mg kg^{-1} amphetamine for behavioral testing of supersensitivity (Supplementary Figure S17a). Afterwards, animals received another high dose of amphetamine and 24 h later the mPFC and dStr were dissected and the insoluble proteome was purified and probed for Disc1. Although we could not detect a difference in Disc1 aggregation in the mPFC, we observed decreased insoluble Disc1 in the dStr upon DA depletion (Supplementary Figure S17b and d). According to these results, the presence of endogenous insoluble Disc1 is correlated with cytosolic DA levels in wild type rats.

DISCUSSION

We present the first transgenic rat model for one of the best-characterized genes implicated in mental illness, *DISC1*. We demonstrate that modest overexpression of full-length human DISC1 causes DISC1 misassembly and a signature of neuropathological, biochemical and behavioral phenotypes involving the dopamine system.

DISC1 is a gene for which mutations or polymorphisms have been associated with chronic mental illnesses like schizophrenia, recurrent major depression, bipolar disorder and autism. This highlights the role of DISC1 as a general vulnerability factor for behavioral control that is not restricted to one specific mental illness, despite its name.[4,5,14] Here, we present a novel mechanism by which full-length DISC1 protein without genetically linked mutations may have a role in a subset of sporadic cases of chronic mental illness, cases where a clear and unambiguous genetic basis cannot be determined. Protein pathology, that is, misassembly of

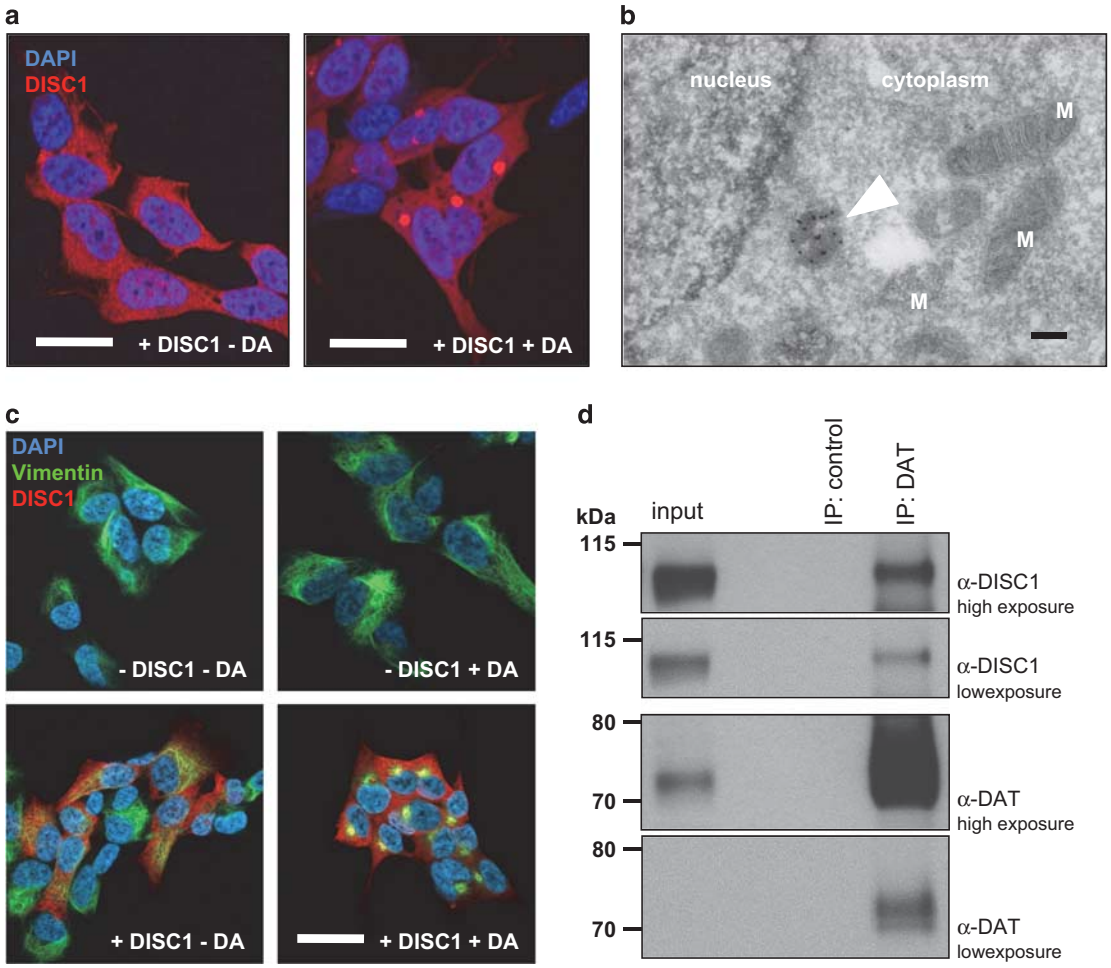

Figure 4. Dopamine-induced DISC1 aggresome formation in cell models. (**a**) Confocal immunofluorescence light microscopy of SH-SY5Y human neuroblastoma cells induced for expression of full-length human DISC1 (S704, L607). DISC1 was diffusely expressed throughout the cytoplasm (left panel). Upon DA treatment (100 μM for 24 h; right panel) the previously diffusely distributed DISC1 built up aggresomes inside the cell. Bar 20 μm. (**b**) Cryoimmunogold electron microscopy for cells from **a**. Arrow marks the perinuclear, immunolabeled dopamine-induced DISC1 aggresome. Bar 100 nm. (**c**) Characterization of dopamine-induced DISC1 aggresomes as shown in **a**. Double-staining shows that DA-induced DISC1 aggresomes (red) are caged by vimentin (green). Bar 20 μm. (**d**) Co-immunoprecipitation of DISC1 by DAT in the tgDISC1 rat brain. In a plasma membrane preparation of the striatum the DAT antibody co-immunoprecipitated transgenic human DISC1. Upper two panels show DISC1 signal, lower two panels DAT signal at two different exposure times. DA, dopamine; DISC1, Disrupted-in-Schizophrenia 1; M, mitochondrion.

a gene product, is an established mechanism in chronic brain diseases like Alzheimer's disease, Parkinson's disease and other neurodegenerative disorders,[18] as well as several non-brain diseases.[59] In addition, protein assembly to large, ordered complexes occurs physiologically and plays important functional roles, including synapse maintenance.[19,60] DISC1 misassembly in tgDISC1 rats led to a signature of biochemical and behavioral phenotypes involving the dopamine system. These phenotypes correspond to phenotypes that are also observed in schizophrenia, such as amphetamine sensitization and the switch from low-affinity to high-affinity D2 receptors.[52] Therefore, we present a novel animal model with high face validity that is relevant for a significant subset of human cases with DISC1-dependent mental illness, tentatively termed DISC1opathies.[61]

In the tgDISC1 rat, we chose to overexpress full-length DISC1 containing the C704 and F607 polymorphisms because they increase aggregation propensity in cell-free *in vitro* systems.[6,7] Both polymorphisms are common alleles that do not predict mental illness as opposed to mutations. Therefore, when evaluating the potential contribution of these polymorphisms on the observed phenotypes, genetic and protein aggregation effects cannot be separated because both phenomena are linked. Furthermore, when expressed in cells, aggregation propensity of the DISC1 protein seems to override effects of polymorphisms (Supplementary Figure S9).

In addition to prominent amphetamine supersensitivity, the hyperexploratory behavior and rotarod deficits can also be related to subtle alterations in the striatal dopaminergic system, which is essential for motor control, reward-related behaviors and exploration. The dStr acts as a convergence point for inputs from the basal ganglia, cortex and thalamus. From the dStr, the direct and indirect pathways arise and exert opposing control over motor function. This is mediated by D1R- and D2R-expressing MSNs that, respectively, promote or inhibit locomotion and exploration.[62] Both pathways are thought to be partially intertwined[63,64] and are affected by dopaminergic input to the dStr. Increased striatal dopamine reduces the excitability of D2R-MSNs and favors locomotion and exploration by weakening the indirect pathway.[65,66] Our results indicate a subtle enhancement of D2R-mediated neurotransmission in tgDISC1 rats: the large (80%) increase in D2High receptors suggests amplification of D2R signaling that is probably not compensated by the modest

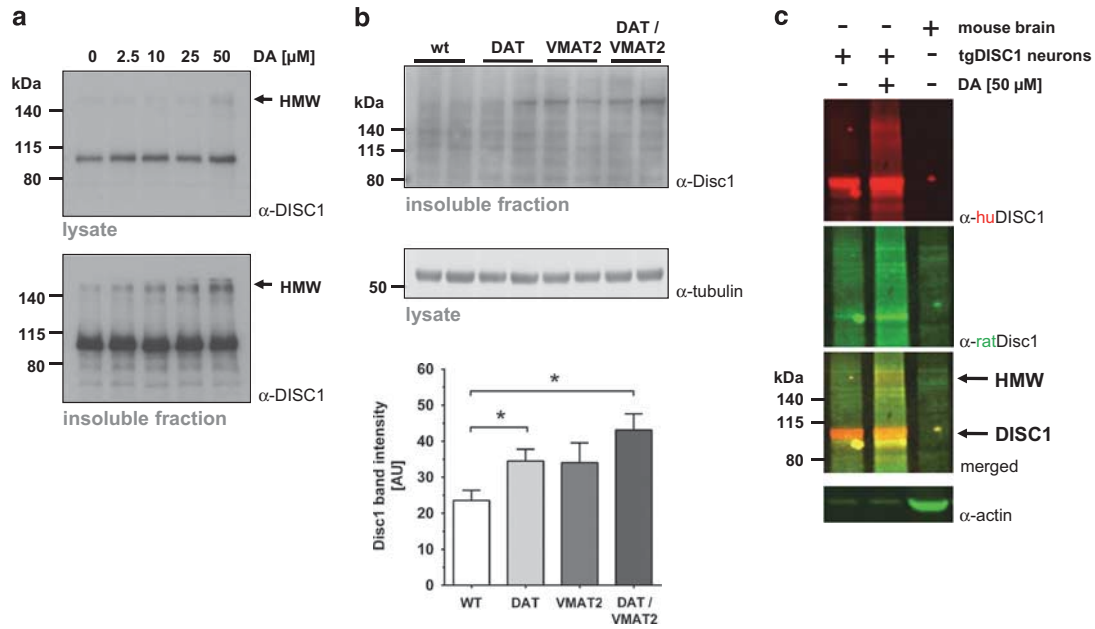

Figure 5. Dopamine-induced DISC1 high-molecular-weight (HMW) bands in cell and animal models. (**a**) Appearance of DISC1 HMW bands upon DA-treatment of cells. Western blot of the lysate (upper panel) or insoluble fraction (lower panel) of NLF human neuroblastoma cells transiently transfected with full-length DISC1 (S704, L607) and treated with DA at indicated concentrations. HMW DISC1-immunoreactive bands appear (arrow) with increasing concentrations of DA. (**b**) Analysis of the purified insoluble fraction of the mPFC of three transgenic mouse lines either overexpressing DAT (DAT-OE), with decreased VMAT2 expression (VMAT2-DE) and double transgenics (DAT-OE:VMAT2-DE). In the western blot (upper panel) a HMW Disc1 signal is visible in all transgenic mouse lines, but not in wild-type mice. As a loading control of the input material for the insoluble fraction preparation homogenates were blotted and incubated with beta-actin on a separate blot. Densitometric quantitation (lower panel) of insoluble HMW Disc1 in the mPFC of transgenic mice shows that while VMAT-DE animals exhibit a trend towards increased Disc1 aggregation in mPFC, in DAT-OE mice Disc1 aggregates were significantly elevated. DAT-OE:VMAT2-DE mice displayed nearly double the amount of Disc1 aggregates in mPFC compared with WT animals (Kruskal-Wallis with one-tailed Dunn's *post hoc* test; DAT-OE: $^*P = 0.029$; DAT-OE:VMAT2-DE: $^*P = 0.014$; $n = 4$ each). (**c**) Western blots of the purified insoluble fraction showing the HMW band as a common signature of DA-induced aggregation of human, rat, and mouse DISC1. Depicted are the insoluble fractions of primary rat cortical neurons derived from tgDISC1 rats with (+) and without (−) incubation with 50 μM dopamine and of endogenous Disc1 from DAT-OE mouse brain, stained with the huDISC1 specific mAB 14F2 (green) and rodent Disc1 specific polyclonal C-term Ab (red), detecting human transgenic and endogenous mouse DISC1, respectively. Primary neuron samples show a dopamine induction-dependent, HMW immunoreactive band above 200 kDa (upper arrow) for endogenous rat as well as transgenic human DISC1. Also endogenous mouse Disc1 shows HMW bands in the insoluble fraction. The actin control demonstrates equal protein content for the lysate input of primary neurons. All means ± s.e.m.

increase in dopamine clearance by DAT. Overall, this would lead to increased D2R-MSN activation promoting hyperexploration in tgDISC1 rats. This might also explain the rotarod deficits in these animals as motor learning is mediated by D2R-MSNs and can be disrupted by exploratory distraction as shown by cell-type specific striatal lesion studies.[67] Mutations in the *DISC1* gene have been linked to aberrant dopamine-related functions. Amphetamine supersensitivity was observed in mouse mutants and in transgenic mice expressing C-terminal deleted DISC1 (1–597).[23,24,26] Also in these transgenic mice, changes were subtle as similar basal DA levels were detected in the dStr.[23,26] Although the Disc1 (L100P) mutant mouse showed elevated D2High receptors in the dStr,[23] the transgenic mouse expressing C-terminal deleted DISC1 showed more D2R and DAT in the dStr.[24] DA-related behavioral and biochemical phenotypes have consistently been found in *Disc1* mouse mutants and transgenic mice expressing mutant *DISC1* gene. Given that partial *Disc1* knockout or localized Disc1 silencing[25] as well as overexpression of non-mutant DISC1 (as shown here) both lead to DA-related phenotypes, it appears that DISC1 protein expression has to be tightly regulated within a narrow range to maintain functional dopamine homeostasis. Thus, DISC1 integrity as well as expression levels seem to have a critical role in dopamine homeostasis.

Our demonstration of a reciprocal relationship between DISC1 misassembly and the major neuromodulator dopamine was unexpected. Unlike other neurotransmitters, cytosolic dopamine is a highly reactive oxidant[68] and is able to induce or accentuate oxidative damage. The suggested connection between DISC1 assembly, DAT function, and cytosolic dopamine could therefore have an important role in controlling cellular stress. We postulate that DISC1 assembly / misassembly could act as a molecular sensor for cellular oxidative stress. Whether the observed DISC1 aggregates[20,21] are archaic remnants of oxidative stress events should be further explored.

In summary, our investigations reveal significant functions of DISC1 in two major regulators of dopamine homeostasis: D2R affinity and DAT activity. Modest DISC1 overexpression in the tgDISC1 rat causes changes in DISC1 assembly that directly impacts dopamine homeostasis in the absence of genetic mutations. Thus, we have identified a novel mechanism of DISC1 pathology involving protein insolubility that was previously underappreciated as a potential risk factor for mental illness.

CONFLICT OF INTEREST

The authors declare no conflict of interest.

ACKNOWLEDGMENTS

CK was supported by grants from the Deutsche Forschungsgemeinschaft (Ko1679/3-1, 4/1), NEURON-ERANET DISCover (BMBF 01EW1003), a NARSAD/BBR Independent Investigator Award (#20350), and EU-FP7 MC-ITN IN-SENS (#607616). FL was

supported by the Canadian Institutes for Health Research. Pamela O'Rorke, Desmond O'Rorke, and Janet Marsh Frosst supported PS work in memory of John William Medland. AM-S was supported by a grant from the Forschungskommission of the Heinrich-Heine University Düsseldorf Medical Faculty (54/2013). MA de Souza Silva was supported by a Heisenberg Fellowship SO 1032/5-1 and EU-FP7 (MC-ITN-IN-SENS- #607616). JPH was supported by NEURON-ERANET DISCover. NIH Grants ES019776 (GWM), NS084739 (KML), DA037653 and ES012870 to (KAS). We thank Franziska Wedekind for excellent technical assistance and helpful discussions regarding autoradiography. We thank Thomas Guillot for construction of the fast-scan cyclic voltammetry system, and members of the HHU Animal Facility for technical assistance.

REFERENCES

1 Millar JK, Wilson-Annan JC, Anderson S, Christie S, Taylor MS, Semple CA *et al.* Disruption of two novel genes by a translocation co-segregating with schizophrenia. *Hum Mol Genet* 2000; **9**: 1415–1423.
2 Blackwood DH, Fordyce A, Walker MT St, Clair DM, Porteous DJ, Muir WJ. Schizophrenia and affective disorders--cosegregation with a translocation at chromosome 1q42 that directly disrupts brain-expressed genes: clinical and P300 findings in a family. *Am J Hum Genet* 2001; **69**: 428–433.
3 St Clair D, Blackwood D, Muir W, Carothers A, Walker M, Spowart G *et al.* Association within a family of a balanced autosomal translocation with major mental illness. *Lancet* 1990; **336**: 13–16.
4 Chubb JE, Bradshaw NJ, Soares DC, Porteous DJ, Millar JK. The DISC locus in psychiatric illness. *Mol Psychiatry* 2008; **13**: 36–64.
5 Bradshaw NJ, Porteous DJ. DISC1-binding proteins in neural development, signalling and schizophrenia. *Neuropharmacology* 2012; **62**: 1230–1241.
6 Leliveld SR, Hendriks P, Michel M, Sajnani G, Bader V, Trossbach S *et al.* Oligomer assembly of the C-terminal DISC1 domain (640-854) is controlled by self-association motifs and disease-associated polymorphism S704C. *Biochemistry* 2009; **48**: 7746–7755.
7 Narayanan S, Arthanari H, Wolfe MS, Wagner G. Molecular characterization of disrupted in schizophrenia-1 risk variant S704C reveals the formation of altered oligomeric assembly. *J Biol Chem* 2011; **286**: 44266–44276.
8 Clapcote SJ, Lipina TV, Millar JK, Mackie S, Christie S, Ogawa F *et al.* Behavioral phenotypes of Disc1 missense mutations in mice. *Neuron* 2007; **54**: 387–402.
9 Koike H, Arguello PA, Kvajo M, Karayiorgou M, Gogos JA. Disc1 is mutated in the 129S6/SvEv strain and modulates working memory in mice. *Proc Natl Acad Sci USA* 2006; **103**: 3693–3697.
10 Shen S, Lang B, Nakamoto C, Zhang F, Pu J, Kuan SL *et al.* Schizophrenia-related neural and behavioral phenotypes in transgenic mice expressing truncated Disc1. *J Neurosci* 2008; **28**: 10893–10904.
11 Kuroda K, Yamada S, Tanaka M, Iizuka M, Yano H, Mori D *et al.* Behavioral alterations associated with targeted disruption of exons 2 and 3 of the Disc1 gene in the mouse. *Hum Mol Genet* 2011; **20**: 4666–4683.
12 Pletnikov MV, Ayhan Y, Nikolskaia O, Xu Y, Ovanesov MV, Huang H *et al.* Inducible expression of mutant human DISC1 in mice is associated with brain and behavioral abnormalities reminiscent of schizophrenia. *Mol Psychiatry* 2008; **13**: 115.
13 Hikida T, Jaaro-Peled H, Seshadri S, Oishi K, Hookway C, Kong S *et al.* Dominant-negative DISC1 transgenic mice display schizophrenia-associated phenotypes detected by measures translatable to humans. *Proc Natl Acad Sci USA* 2007; **104**: 14501–14506.
14 Brandon NJ, Sawa A. Linking neurodevelopmental and synaptic theories of mental illness through DISC1. *Nat Rev Neurosci* 2011; **12**: 707–722.
15 Porteous DJ, Thomson PA, Millar JK, Evans KL, Hennah W, Soares DC *et al.* DISC1 as a genetic risk factor for schizophrenia and related major mental illness: response to Sullivan. *Mol Psychiatry* 2014; **19**: 141–143.
16 Sullivan PF. Questions about DISC1 as a genetic risk factor for schizophrenia. *Mol Psychiatry* 2013; **18**: 1050–1052.
17 Bertram L, Lill CM, Tanzi RE. The genetics of Alzheimer disease: back to the future. *Neuron* 2010; **68**: 270–281.
18 Prusiner SB. Shattuck Lecture—neurodegenerative diseases and prions. *N Engl J Med* 2001; **344**: 1516–1526.
19 Greenwald J, Riek R. Biology of amyloid: structure, function, and regulation. *Structure* 2010; **18**: 1244–1260.
20 Leliveld SR, Bader V, Hendriks P, Prikulis I, Sajnani G, Requena JR *et al.* Insolubility of disrupted-in-schizophrenia 1 disrupts oligomer-dependent interactions with nuclear distribution element 1 and is associated with sporadic mental disease. *J Neurosci* 2008; **28**: 3839–3845.
21 Ottis P, Bader V, Trossbach S, Kretzschmar H, Michel M, Leliveld SR *et al.* Convergence of two independent mental disease genes on the protein level: recruitment of dysbindin to cell invasive DISC1 aggresomes. *Biol Psychiatry* 2011; **70**: 604–610.
22 Lipina TV, Roder JC. Disrupted-In-Schizophrenia-1 (DISC1) interactome and mental disorders: impact of mouse models. *Neurosci Biobehav Rev* 2014; **45**: 271–294.
23 Lipina TV, Niwa M, Jaaro-Peled H, Fletcher PJ, Seeman P, Sawa A *et al.* Enhanced dopamine function in DISC1-L100P mutant mice: implications for schizophrenia. *Genes Brain Behav* 2010; **9**: 777–789.
24 Jaaro-Peled H, Niwa M, Foss CA, Murai R, de Los Reyes S, Kamiya A *et al.* Subcortical dopaminergic deficits in a DISC1 mutant model: a study in direct reference to human molecular brain imaging. *Hum Mol Genet* 2013; **22**: 1574–1580.
25 Niwa M, Kamiya A, Murai R, Kubo K, Gruber AJ, Tomita K *et al.* Knockdown of DISC1 by in utero gene transfer disturbs postnatal dopaminergic maturation in the frontal cortex and leads to adult behavioral deficits. *Neuron* 2010; **65**: 480–489.
26 Ayhan Y, Abazyan B, Nomura J, Kim R, Ladenheim B, Krasnova IN *et al.* Differential effects of prenatal and postnatal expressions of mutant human DISC1 on neurobehavioral phenotypes in transgenic mice: evidence for neurodevelopmental origin of major psychiatric disorders. *Mol Psychiatry* 2011; **16**: 293–306.
27 Pogorelov VM, Nomura J, Kim J, Kannan G, Ayhan Y, Yang C *et al.* Mutant DISC1 affects methamphetamine-induced sensitization and conditioned place preference: a comorbidity model. *Neuropharmacology* 2012; **62**: 1242–1251.
28 Nakai T, Nagai T, Wang R, Yamada S, Kuroda K, Kaibuchi K *et al.* Alterations of GABAergic and dopaminergic systems in mutant mice with disruption of exons 2 and 3 of the Disc1 gene. *Neurochem Int* 2014; **74**: 74–83.
29 Su P, Li S, Chen S, Lipina TV, Wang M, Lai TK *et al.* A dopamine D2 receptor-DISC1 protein complex may contribute to antipsychotic-like effects. *Neuron* 2014; **84**: 1302–1316.
30 Scott MR, Kohler R, Foster D, Prusiner SB. Chimeric prion protein expression in cultured cells and transgenic mice. *Protein Sci* 1992; **1**: 986–997.
31 Masoud ST, Vecchio LM, Bergeron Y, Hossain MM, Nguyen LT, Bermejo MK *et al.* Increased expression of the dopamine transporter leads to loss of dopamine neurons, oxidative stress and l-DOPA reversible motor deficits. *Neurobiol Dis* 2015; **74**: 66–75.
32 Salahpour A, Ramsey AJ, Medvedev IO, Kile B, Sotnikova TD, Holmstrand E *et al.* Increased amphetamine-induced hyperactivity and reward in mice overexpressing the dopamine transporter. *Proc Natl Acad Sci USA* 2008; **105**: 4405–4410.
33 Caudle WM, Richardson JR, Wang MZ, Taylor TN, Guillot TS, McCormack AL *et al.* Reduced vesicular storage of dopamine causes progressive nigrostriatal neurodegeneration. *J Neurosci* 2007; **27**: 8138–8148.
34 Mooslehner KA, Chan PM, Xu W, Liu L, Smadja C, Humby T *et al.* Mice with very low expression of the vesicular monoamine transporter 2 gene survive into adulthood: potential mouse model for parkinsonism. *Mol Cell Biol* 2001; **21**: 5321–5331.
35 Bermejo MK, Milenkovic M, Salahpour A, Ramsey AJ. Preparation of synaptic plasma membrane and postsynaptic density proteins using a discontinuous sucrose gradient. *J Vis Exp* 2014; **91**: e51896.
36 Ramsey AJ, Milenkovic M, Oliveira AF, Escobedo-Lozoya Y, Seshadri S, Salahpour A *et al.* Impaired NMDA receptor transmission alters striatal synapses and DISC1 protein in an age-dependent manner. *Proc Natl Acad Sci USA* 2011; **108**: 5795–5800.
37 Seeman P, Guan HC. Glutamate agonist LY404,039 for treating schizophrenia has affinity for the dopamine D2(High) receptor. *Synapse* 2009; **63**: 935–939.
38 Shuto T, Seeman P, Kuroiwa M, Nishi A. Repeated administration of a dopamine D1 receptor agonist reverses the increased proportions of striatal dopamine D1High and D2High receptors in methamphetamine-sensitized rats. *Eur J Neurosci* 2008; **27**: 2551–2557.
39 Pum ME, Schable S, Harooni HE, Topic B, De Souza Silva MA, Li JS *et al.* Effects of intranasally applied dopamine on behavioral asymmetries in rats with unilateral 6-hydroxydopamine lesions of the nigro-striatal tract. *Neuroscience* 2009; **162**: 174–183.
40 Peters PJ, Bos E, Griekspoor A. Cryo-immunogold electron microscopy. *Curr Protoc Cell Biol* 2006; **Chapter 4**: Unit 47.
41 Wang Q, Charych EI, Pulito VL, Lee JB, Graziane NM, Crozier RA *et al.* The psychiatric disease risk factors DISC1 and TNIK interact to regulate synapse composition and function. *Mol Psychiatry* 2011; **16**: 1006–1023.
42 Torrey EF, Webster M, Knable M, Johnston N, Yolken RH. The stanley foundation brain collection and neuropathology consortium. *Schizophr Res* 2000; **44**: 151–155.
43 Johnstone M, Thomson PA, Hall J, McIntosh AM, Lawrie SM, Porteous DJ. DISC1 in schizophrenia: genetic mouse models and human genomic imaging. *Schizophr Bull* 2011; **37**: 14–20.
44 Seshadri S, Kamiya A, Yokota Y, Prikulis I, Kano S, Hayashi-Takagi A *et al.* Disrupted-in-Schizophrenia-1 expression is regulated by beta-site amyloid precursor protein cleaving enzyme-1-neuregulin cascade. *Proc Natl Acad Sci USA* 2010; **107**: 5622–5627.
45 Hsiao KK, Borchelt DR, Olson K, Johannsdottir R, Kitt C, Yunis W *et al.* Age-related CNS disorder and early death in transgenic FVB/N mice overexpressing Alzheimer amyloid precursor proteins. *Neuron* 1995; **15**: 1203–1218.

46 Chishti MA, Yang DS, Janus C, Phinney AL, Horne P, Pearson J *et al.* Early-onset amyloid deposition and cognitive deficits in transgenic mice expressing a double mutant form of amyloid precursor protein 695. *J Biol Chem* 2001; **276**: 21562–21570.
47 Manson J, West JD, Thomson V, McBride P, Kaufman MH, Hope J. The prion protein gene: a role in mouse embryogenesis? *Development* 1992; **115**: 117–122.
48 Schurov IL, Handford EJ, Brandon NJ, Whiting PJ. Expression of disrupted in schizophrenia 1 (DISC1) protein in the adult and developing mouse brain indicates its role in neurodevelopment. *Mol Psychiatry* 2004; **9**: 1100–1110.
49 Nakata K, Lipska BK, Hyde TM, Ye T, Newburn EN, Morita Y *et al.* DISC1 splice variants are upregulated in schizophrenia and associated with risk polymorphisms. *Proc Natl Acad Sci USA* 2009; **106**: 15873–15878.
50 van Haren NE, Cahn W, Hulshoff Pol HE, Kahn RS. Schizophrenia as a progressive brain disease. *Eur Psychiatry* 2008; **23**: 245–254.
51 Lieberman JA, Kane JM, Alvir J. Provocative tests with psychostimulant drugs in schizophrenia. *Psychopharmacology (Berl)* 1987; **91**: 415–433.
52 Seeman P, Schwarz J, Chen JF, Szechtman H, Perreault M, McKnight GS *et al.* Psychosis pathways converge via D2high dopamine receptors. *Synapse* 2006; **60**: 319–346.
53 Seeman P. Schizophrenia and dopamine receptors. *Eur Neuropsychopharmacol* 2013; **23**: 999–1009.
54 Kopito RR. Aggresomes, inclusion bodies and protein aggregation. *Trends Cell Biol* 2000; **10**: 524–530.
55 Levin EC, Acharya NK, Sedeyn JC, Venkataraman V, D'Andrea MR, Wang HY *et al.* Neuronal expression of vimentin in the Alzheimer's disease brain may be part of a generalized dendritic damage-response mechanism. *Brain Res* 2009; **1298**: 194–207.
56 Soderberg O, Gullberg M, Jarvius M, Ridderstrale K, Leuchowius KJ, Jarvius J *et al.* Direct observation of individual endogenous protein complexes in situ by proximity ligation. *Nat Methods* 2006; **3**: 995–1000.
57 Featherstone RE, Kapur S, Fletcher PJ. The amphetamine-induced sensitized state as a model of schizophrenia. *Prog Neuropsychopharmacol Biol Psychiatry* 2007; **31**: 1556–1571.
58 Kahlig KM, Galli A. Regulation of dopamine transporter function and plasma membrane expression by dopamine, amphetamine, and cocaine. *Eur J Pharmacol* 2003; **479**: 153–158.
59 Blancas-Mejia LM, Ramirez-Alvarado M. Systemic amyloidoses. *Annu Rev Biochem* 2013; **82**: 745–774.
60 Si K, Choi YB, White-Grindley E, Majumdar A, Kandel ER. Aplysia CPEB can form prion-like multimers in sensory neurons that contribute to long-term facilitation. *Cell* 2010; **140**: 421–435.
61 Korth C. DISCopathies: brain disorders related to DISC1 dysfunction. *Rev Neurosci* 2009; **20**: 321–330.
62 Kravitz AV, Freeze BS, Parker PR, Kay K, Thwin MT, Deisseroth K *et al.* Regulation of parkinsonian motor behaviours by optogenetic control of basal ganglia circuitry. *Nature* 2010; **466**: 622–626.
63 Calabresi P, Picconi B, Tozzi A, Ghiglieri V, Di Filippo M. Direct and indirect pathways of basal ganglia: a critical reappraisal. *Nat Neurosci* 2014; **17**: 1022–1030.
64 Cazorla M, de Carvalho FD, Chohan MO, Shegda M, Chuhma N, Rayport S *et al.* Dopamine D2 receptors regulate the anatomical and functional balance of basal ganglia circuitry. *Neuron* 2014; **81**: 153–164.
65 Surmeier DJ, Ding J, Day M, Wang Z, Shen W. D1 and D2 dopamine-receptor modulation of striatal glutamatergic signaling in striatal medium spiny neurons. *Trends Neurosci* 2007; **30**: 228–235.
66 Simpson EH, Kellendonk C, Kandel E. A possible role for the striatum in the pathogenesis of the cognitive symptoms of schizophrenia. *Neuron* 2010; **65**: 585–596.
67 Durieux PF, Schiffmann SN, de Kerchove d'Exaerde A. Differential regulation of motor control and response to dopaminergic drugs by D1R and D2R neurons in distinct dorsal striatum subregions. *EMBO J* 2012; **31**: 640–653.
68 Sulzer D, Chen TK, Lau YY, Kristensen H, Rayport S, Ewing A. Amphetamine redistributes dopamine from synaptic vesicles to the cytosol and promotes reverse transport. *J Neurosci* 1995; **15**: 4102–4108.

Supplementary Information accompanies the paper on the Molecular Psychiatry website (http://www.nature.com/mp)